

Am(III)/Nd(III) INTERACTIONS WITH BORATE: EXPERIMENTAL INVESTIGATIONS OF Nd(OH)₃(micro cr) SOLUBILITY IN NaCl SOLUTIONS IN EQUILIBRIUM WITH BORAX

Yongliang Xiong^{1)*}, Leslie Kirkes¹⁾, Cassie Marrs¹⁾, Jandi Knox¹⁾

¹⁾ Sandia National Laboratories (SNL), Carlsbad Programs Group, 4100 National Parks Highway, Carlsbad, NM 88220, USA

ABSTRACT– In previous studies on Am(III)/Nd(III) interactions with borate, the borate concentrations were kept at a relatively low level, up to $\sim 0.16 \text{ mol}\cdot\text{kg}^{-1}$ as the highest. Such concentrations of borate are not saturated, in terms of borate, with borate-bearing phases such as borax ($\text{Na}_2\text{B}_4\text{O}_7\cdot 10\text{H}_2\text{O}$) and tinalconite ($\text{Na}_2\text{B}_4\text{O}_7\cdot 5\text{H}_2\text{O}$) that could be present in geological repositories. For instance, tinalconite has been observed as a corrosion product for borosilicate glass for HLW under the repository conditions in China.

In this study, we examine the Nd(III) interactions with borate in equilibrium with borax in a wide range of NaCl solutions at 25°C. In our experiments, the solubility-controlling phase for Nd(III) is Nd(OH)₃(micro cr). In synthesis of Nd(OH)₃(micro cr), we followed the procedure from literature. Our results indicate that high borate concentrations ($\sim 0.5 \text{ mol}\cdot\text{kg}^{-1}$) in 0.01 and 0.1 $\text{mol}\cdot\text{kg}^{-1}$ NaCl solutions have an obvious effect on Nd(III). At such a high concentration of borate, borate can enhance the solubility of Nd(OH)₃(micro cr), or NdB₉O₁₃(OH)₄(cr) may control the solubility.

1. Introduction

Borate is important to geological processes, although boron is the 41st abundant element in the Earth's Crust, lower than the abundances of rare earth elements such as Nd, which is the 28th abundant element. In natural groundwaters such as brines associated with salt formations, there may be relatively high concentrations of borate [1]. In addition, when borosilicate glass for high level nuclear waste (HLW) is corroded, borate is also released into the groundwater [2-3]. Borate can impact nuclear waste management in two aspects. First of all, borate can form an aqueous complex with Nd(III) and Eu(III) [4-6], analogs to actinides in +III oxidation state, such as Am(III). Therefore, borate could become a potential transport agent for actinides if the Am(III)-borate complex contributes significantly to the total Am(III) concentrations. In the second aspect, numerous actinide borates have recently been successfully synthesized [7-8], including a Pu(III) borate, Pu₂[B₁₂O₁₈(OH)₄Br₂(H₂O)₃] $\cdot 0.5\text{H}_2\text{O}$, in addition to the well known lanthanide borates such as NdB₉O₁₃(OH)₄ [9]. This implies that actinides in waste could be transformed into, or be sequestered as, actinide borates, if their solubility limits are reached.

Actinides in +III state represented by Am(III) are present in nuclear waste in geological

repositories. Therefore, the interactions between Am(III) and borate are important for performance assessment (PA) for geological repositories for nuclear wastes. As an example, in the Waste Isolation Pilot Plant (WIPP), a U.S. DOE geological repository for defense-related transuranic (TRU) waste in the bedded salt formations in New Mexico, USA, the inventory of Am(III) in waste was 143 kg for the WIPP Compliance Application Re-Certification in 2009 (CRA-2009). The borate concentrations in the two WIPP brines that are important for performance assessment (PA), i.e., Generic Weep Brine (GWB), and Energy Research and Development Administration (WIPP Well) 6 (ERDA-6), are $0.180 \text{ mol}\cdot\text{kg}^{-1}$ and $0.0692 \text{ mol}\cdot\text{kg}^{-1}$ [10], respectively.

In the previous studies on Am(III)/Nd(III) interactions with borate, the borate concentrations were kept at the relatively low level, and up to $\sim 0.16 \text{ mol}\cdot\text{kg}^{-1}$ as the highest (i.e., [4, 9]). Such concentrations of borate are not saturated, in terms of borate, with borate-bearing phases such as borax ($\text{Na}_2\text{B}_4\text{O}_7\cdot 10\text{H}_2\text{O}$) and tinalconite ($\text{Na}_2\text{B}_4\text{O}_7\cdot 5\text{H}_2\text{O}$) that could be present in geological repositories. For instance, tinalconite has been observed as one of corrosion products for borosilicate glass for HLW under the repository conditions in China [11]. The borate concentrations saturated with borax and

tincalconite are much higher than $0.16 \text{ mol}\cdot\text{kg}^{-1}$, especially in solutions with low concentrations of sodium. For example, the borate concentrations are $\sim 0.5 \text{ mol}\cdot\text{kg}^{-1}$ in $0.01 \text{ mol}\cdot\text{kg}^{-1}$, NaCl [12]. Therefore, the Am(III)/Nd(III) interactions with borate need to be further studied, especially in high borate concentrations.

2. Methods and Results

In this section we describe the experimental methodology used in this study.

2.1 Synthesis of Starting Material

As detailed in Wood et al. [13], many other synthesis methods suffer from various shortcomings, which would result in difficulty/uncertainty interpreting solubility data. Therefore, starting with well-defined high-purity material is of fundamental importance to the success of solubility experiments. In synthesis of $\text{Nd}(\text{OH})_3(\text{micro cr})$, high purity Nd_2O_3 was first loaded into Paar® reaction vessels with deaerated DI water, and then the reaction vessels were sealed in a glovebox under a positive pressure of an inert gas. The reaction vessels were then removed from the glovebox and placed into a muffle furnace. $\text{Nd}(\text{OH})_3(\text{micro cr})$ was synthesized by reacting the high purity Nd_2O_3 with the deaerated DI water at 473.15 K in Paar® reaction vessels for a period of two weeks. Following the synthesis step, the reaction vessels were then transferred back into the glovebox, and were opened for drying in an atmosphere of inert gas. This synthesis method assures the complete conversion of Nd_2O_3 to $\text{Nd}(\text{OH})_3(\text{micro cr})$, as demonstrated by XRD and SEM-EDS characterizations. The SEM-EDS characterization shows that the size of crystals is small, and the majority of crystals are around micrometer or sub-micrometer in size, as indicated by SEM-EDS images (Figure 1A and 1B). As shown by the XRD analysis, the synthetic neodymium has a well-defined XRD pattern (Figure 2) that is indicative of a crystalline phase. Therefore, we term our synthetic neodymium hydroxide as “micro crystalline neodymium hydroxide”, $\text{Nd}(\text{OH})_3(\text{micro cr})$, throughout the entire paper. Figure 2 shows that the XRD pattern of synthetic $\text{Nd}(\text{OH})_3(\text{micro cr})$ produced by this work has the exact match with the reference

standard of $\text{Nd}(\text{OH})_3(\text{cr})$ from the International Center of Diffraction Data (ICDD).

Of note, the deaerated DI water used in the synthesis was prepared by vigorously bubbling high purity Ar or N_2 gas through DI water for a minimum of 30 minutes in the glovebox, following a similar procedure used by Xiong [14]. This deaeration process was intended to remove any dissolved CO_2 and therefore ensure the synthesis process was not contaminated by carbonate.

2.2 Experimental Setup

Undersaturation experiments are conducted at $298.15 \pm 0.5 \text{ K}$. In our solubility experiments, approximately 0.3 grams of $\text{Nd}(\text{OH})_3(\text{micro cr})$ and about 10 grams of $\text{Na}_2\text{B}_4\text{O}_7\cdot 10\text{H}_2\text{O}$ (borax) were placed into serum bottles along with 100 mL of supporting solutions with the desired ionic strength. The supporting solutions consisted of 0.01, 0.1, 1.0, 2.1, 3.2, 4.4 and 5.0 $\text{mol}\cdot\text{kg}^{-1}$ NaCl solutions where $\text{mol}\cdot\text{kg}^{-1}$ refers to concentration on molal scale, i.e., moles per 1000 g of water. All supporting solutions were prepared from reagent grade chemicals from Fisher Scientific, or its associated vendors, and deaerated DI water.

Solution samples were periodically withdrawn from the experiments to determine if the system had reached equilibrium. Before each sampling, pH readings were taken for each experiment. In each sampling, about 3 mL of solution samples were taken from each experiment, and the solution samples were filtered through a $0.2 \mu\text{m}$ filter, and transferred into pre-weighed 10 mL Grade A volumetric flasks. After filtration, masses of each solution sample were determined with a balance precise to the fourth decimal place. Samples were then immediately acidified with 0.5 mL of the Optima® Grade HNO_3 from Fisher Scientific, and diluted to 10 mL with DI water. Prior to chemical analyses for Nd using the PerkinElmer NexION 300D ICP-MS, and for Na using the PerkinElmer Optima 3300 Dual View (DV) ICP-AES, aliquots from the afore-mentioned acidified samples were further diluted to an appropriate ionic strength.

The pH readings were measured with an Orion-Ross combination pH glass electrode, coupled with an Orion Research EA 940 pH meter that was calibrated with three pH buffers (pH 4, pH 7, and pH 10). The measured pH readings were converted to negative logarithm of hydrogen ion concentrations on molar scale (i.e., pCH) following

the procedure detailed in Xiong [14] and Xiong and Lord [10], and pH_m 's were converted to pH_m 's (negative logarithm of hydrogen ion concentrations on molar scale) according to the equations in Xiong et al. [15].

2.3 Experimental Results

Our experimental results are displayed in Figures 3-5. In Figures 3-5, our experimental results are compared with the predicted values for $Am(OH)_3(s)$ and $AmB_4O_{13}(OH)_4(cr)$ which were calculated using EQ3/6 Version 8.0a, and the thermodynamic database data0.fm2. Note the dashed and dotted lines in Figures 3-5 represent the EQ3/6 simulated concentrations, and the symbols are the measured data. They are produced using EQ3/6 Version 8.0a [16-17] with the database data0.fm2 [18-19]. EQ3/6 Version 8.0a has been extensively used in the previous publications [e.g., 20-23]. The equilibrium constant for $AmB_9O_{13}(OH)_4(cr)$ at 25°C is from [24].

Figure 3 shows that there are relatively high concentrations of Nd(III) in the experiments in 0.01 and 0.1 mol•kg⁻¹ NaCl. Of note, the borate concentrations saturated with borax in these two experiments are 0.53 and 0.42 mol•kg⁻¹, respectively. The Nd(III) concentrations without the species $AmHB_4O_7^{2+}$ are higher than those predicted for $Am(OH)_3(s)$, but are close to those predicted for $AmB_9O_{13}(OH)_4(cr)$. This may suggest that borate enhances the solubility of $Am(OH)_3(s)$, or $AmB_9O_{13}(OH)_4(cr)$ controls the solubility.

Figure 4 displays the results in 1.0 and 2.1 mol•kg⁻¹ NaCl. In these two experiments, the borate concentrations are 0.22 and 0.18, respectively. Again, the Nd(III) concentrations are higher than those predicted for $Am(OH)_3(s)$, but are close to those for $AmB_9O_{13}(OH)_4(cr)$.

The results in 3.2, 4.4, and 5.0 mol•kg⁻¹ appear in Figure 5. The Nd(III) concentrations are close to those predicted for $Am(OH)_3(s)$. It implies that the role that borate plays to enhance the solubility of $Am(OH)_3(s)$ is less at high NaCl concentrations. The borate concentrations in these experiments are 0.20, 0.16 and 0.16 mol•kg⁻¹, respectively.

It is of interest to note that the data from Hinz et al. [9] for $NdB_9O_{13}(OH)_4(cr)$ at $pH_m \sim 9$ are close to those predicted for $Am(OH)_3(s)$. As indicated

by Figure 5, $NdB_9O_{13}(OH)_4(cr)$ could be converted to the hydroxide form in high pH_m region.

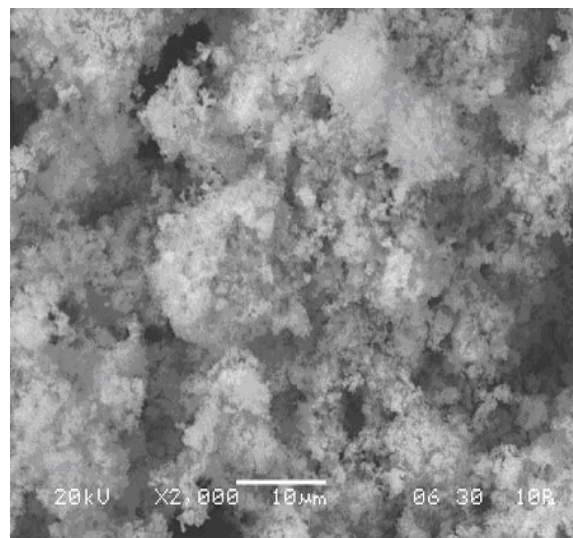


Fig. 1A. SEM image of the starting material used in experiments in this study.

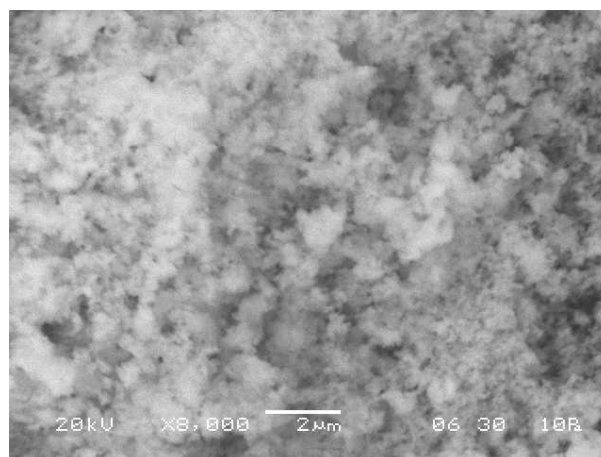


Fig. 1B. SEM image of the starting material used in experiments in this study.

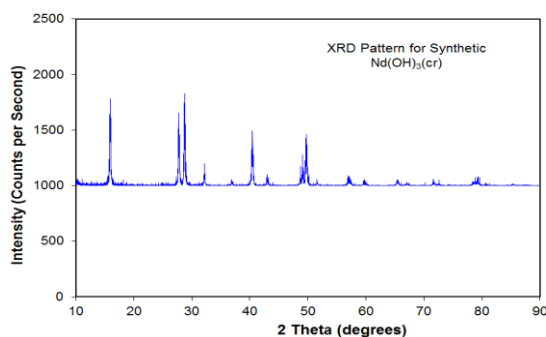


Fig. 2. XRD pattern of $Nd(OH)_3(\text{micro cr})$ used in solubility experiments in this study.

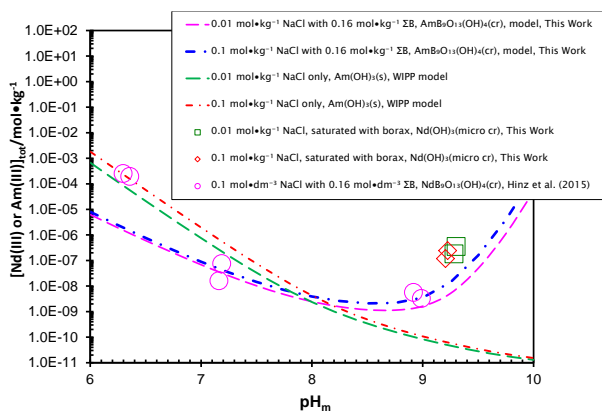


Fig. 3. A plot showing Nd(III)/Am(III) concentrations as a function of pH_m in low ionic strength range.

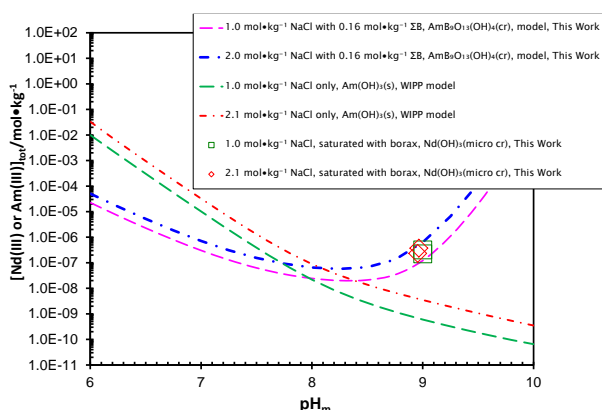


Fig. 4. A plot showing Nd(III)/Am(III) concentrations as a function of pH_m in moderate ionic strength range.

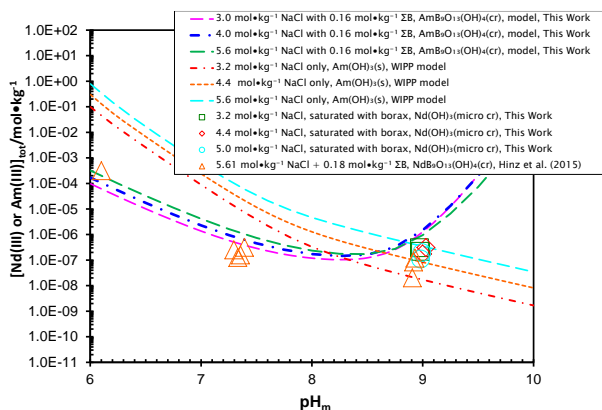


Fig. 5. A plot showing Nd(III)/Am(III) concentrations as a function of pH_m in high ionic strength range.

3. Conclusions

We have conducted solubility measurements regarding $Nd(OH)_3(\text{micro cr})$ in NaCl solutions saturated with borax at 25°C. Our results indicate that high borate concentrations ($\sim 0.5 \text{ mol}\cdot\text{kg}^{-1}$) in 0.01 and $0.1 \text{ mol}\cdot\text{kg}^{-1}$ NaCl solutions have an

obvious effect on Nd(III). At such a high concentration of borate, borate can enhance the solubility of $Nd(OH)_3(\text{micro cr})$, or $NdB_5O_{13}(OH)_4(\text{cr})$ may control the solubility.

4. Acknowledgements

Sandia National Laboratories is a multimission laboratory operated by National Technology and Engineering Solutions of Sandia, LLC., a wholly owned subsidiary of Honeywell International, Inc., for the U.S. Department of Energy's National Nuclear Security Administration under contract DE-NA-0003525. This research is funded by WIPP programs administered by the Office of Environmental Management (EM) of the U.S. Department of Energy. SAND2017-12040C

REFERENCES

1. A.Vengosh, A. Starinsky, Y. Kolodny, and A.R. Chivas, *Geochimica et Cosmochimica Acta* 55, 1689 (1991).
2. T. Advocat, P. Jollivet, J.L. Crovisier, M. del Nero, *Journal of Nuclear Materials* 298, 55 (2001).
3. E. Curti, R. Dahn, F. Farges, and M. Vespa, *Geochimica et Cosmochimica Acta* 73, 2283 (2009)
4. M. Borkowski, M. Richmann, D.T. Reed, and Y.-L. Xiong, Y.-L., *Radiochimica Acta* 98, 577 (2010).
5. J. Schott, J. Kretzschmar, M. Acker, S. Eidner, M.U. Kumke, B. Drobot, A. Barkleit, S. Taut, V. Brendler, and T. Stumpf, T., *Dalton Transactions* 43, 11516 (2014).
6. J. Schott, J. Kretzschmar, S. Tsushima, B. Drobot, M. Acker, A. Barkleit, S. Taut, V. Brendler, and T. Stumpf, T., *Dalton Transactions* 44, 11095 (2015).
7. S.-A.Wang, E.V Alekseev, W. Depmeier, and T.E. Albrecht-Schmitt, *Inorganic Chemistry* 50, 2079 (2010).
8. S.-A.Wang, E.V Alekseev, W. Depmeier, and T.E. Albrecht-Schmitt, *Chemical Communications* 47, 10874 (2011).
9. K. Hinz, M. Altmaier, X. Gaona, T. Rabung, D. Schild, M. Richmann, D.T. Reed, E.V. Alekseev, and H. Geckeis, H., *New journal of chemistry* 39, 849 (2015).
10. Y.-L. Xiong, and A.C.S. Lord, *Applied Geochemistry* 23, 1634 (2008).

11. Zh-T. Zhang, X-Y. Gan, L. Wang, H.-Q. Xing, International Journal of Corrosion, Volume 2012, Article ID 924963 (2012).
12. Y.-L. Xiong, L. Kirkes, T. Westfall, American Mineralogist 98, 2030 (2013).
13. Wood, S.A., D.A. Palmer, D.J. Wesolowski, and P. Bénézeth, The aqueous geochemistry of the rare earth elements and yttrium. Part XI. The solubility of Nd(OH)₃ and hydrolysis of Nd³⁺ from 30 to 290 °C at saturated water vapor pressure with in-situ pH_m measurement. In Hellmann, R. and Wood, S.A., ed., Water-Rock Interactions, Ore Deposits, and Environmental Geochemistry: A Tribute to David Crerar, Special Publication 7, The Geochemical Society, pp. 229–256 (2002).
14. Xiong, Y.-L., Aquatic Geochemistry 14, 223 (2008).
15. Xiong, Y.-L., Deng, H.-R., Nemer, M., and Johnsen, S., Geochimica et Cosmochimica Acta, 74, 4605 (2010).
16. T.W. Wolery, Y.-L. Xiong, and J. J. Long, “Verification and Validation Plan/Validation Document for EQ3/6 Version 8.0a for Actinide Chemistry, Document Version 8.10.” Carlsbad, NM: Sandia National laboratories, ERMS 550239, 2010.
17. Y.-L. Xiong, “WIPP Verification and Validation Plan/Validation Document for EQ3/6 Version 8.0a for Actinide Chemistry, Revision 1, Document Version 8.20. Supersedes ERMS 550239.” Carlsbad, NM. Sandia National Laboratories, ERMS 555358, 2011.
18. P.S. Domski, “Memo AP-173, EQ3/6 Database Update: DATA0.FM2” Memorandum to WIPP Records, October 27, 2015. Carlsbad, NM: Sandia National Laboratories. ERMS 564914, 2015.
19. Y.-L. Xiong, P.S. Domski, P.S., “Updating the WIPP Thermodynamic Database, Revision 1, Supersedes ERMS 565730.” Carlsbad, NM: Sandia National Laboratories. ERMS 566047, 2016.
20. Y.-L. Xiong, Journal of Solution Chemistry 42, 139 (2013).
21. Y.-L. Xiong, American Mineralogist 98, 141 (2013).
22. Y.-L. Xiong, Chemical Geology 373, 37 (2014).
23. Y.-L. Xiong, Monatshefte für Chemie - Chemical Monthly 146, 1433 (2015).
24. Xiong, Y., *MRS Advances*, 2(13), pp.741-746 (2017).